Changes in Brain Resting-state Functional Connectivity Associated with Peripheral Nerve Block

A Pilot Study

M. Stephen Melton, M.D., Jeffrey N. Browndyke, Ph.D., Todd B. Harshbarger, Ph.D., David J. Madden, Ph.D., Karen C. Nielsen, M.D., Stephen M. Klein, M.D.

ABSTRACT

Background: Limited information exists on the effects of temporary functional deafferentation (TFD) on brain activity after peripheral nerve block (PNB) in healthy humans. Increasingly, resting-state functional connectivity (RSFC) is being used to study brain activity and organization. The purpose of this study was to test the hypothesis that TFD through PNB will influence changes in RSFC plasticity in central sensorimotor functional brain networks in healthy human participants.

Methods: The authors achieved TFD using a supraclavicular PNB model with 10 healthy human participants undergoing functional connectivity magnetic resonance imaging before PNB, during active PNB, and during PNB recovery. RSFC differences among study conditions were determined by multiple-comparison–corrected (false discovery rate–corrected *P* value less than 0.05) random-effects, between-condition, and seed-to-voxel analyses using the left and right manual motor regions.

Results: The results of this pilot study demonstrated disruption of *inter*hemispheric left-to-right manual motor region RSFC (*e.g.*, mean Fisher-transformed z [effect size] at pre-PNB 1.05 *vs.* 0.55 during PNB) but preservation of *intra*hemispheric RSFC of these regions during PNB. Additionally, there was increased RSFC between the left motor region of interest (PNB-affected area) and *bilateral* higher order visual cortex regions after clinical PNB resolution (*e.g.*, Fisher z between left motor region of interest and right and left lingual gyrus regions during PNB, –0.1 and –0.6 *vs.* 0.22 and 0.18 after PNB resolution, respectively).

Conclusions: This pilot study provides evidence that PNB has features consistent with other models of deafferentation, making it a potentially useful approach to investigate brain plasticity. The findings provide insight into RSFC of sensorimotor functional brain networks during PNB and PNB recovery and support modulation of the sensory–motor integration feedback loop as a mechanism for explaining the behavioral correlates of peripherally induced TFD through PNB.

(ANESTHESIOLOGY 2016; 125:368-77)

THE term "plasticity" refers to changes in brain activity and organization in response to injury or perceived injury, such as experimental deafferentation. Plasticity associated with temporary and permanent deafferentation has been studied in both animal[1–5] and human subjects.[6–10] In a series of animal studies, Merzenich and colleagues[1–5] demonstrated cortical reorganization with adjacent intact cortical representations "invading" neighboring deafferentated brain regions after experimental nerve transection, digit amputation, and epidural anesthesia. Subsequent work in healthy humans utilizing transient ischemic and pharmacologic nerve block further characterized central reorganization after deafferentation.[6–10] Weiss *et al.*[9] examined central plasticity in the primary somatomotor cortex after radial and median nerve block. Using magnetoencephalographic source imaging and transcranial magnetic stimulation, results of this study documented adaptive plasticity with cortical expansion

What We Already Know about This Topic

- Resting-state functional connectivity determined by functional connectivity magnetic resonance imaging can be used to study brain activity and network organization
- Temporary functional deafferentation, such as that produced by peripheral nerve blocks, can promote adaptive brain plasticity

What This Article Tells Us That Is New

- Using supraclavicular peripheral nerve block (PNB) as a model of temporary functional deafferentation (TFD) in 10 human subjects, functional connectivity magnetic resonance imaging showed disruption of interhemispheric resting-state functional connectivity (RSFC) in the manual motor region but preservation of intrahemispheric RSFC during PNB, with increased RSFC between the affected motor area and bilateral visual cortices upon PNB resolution
- TFD produced by PNB produces similar effects on RSFC as other models, which provides a useful model for TFD-induced changes in neuroplasticity

This article is featured in "This Month in Anesthesiology," page 1A. M.S.M. and J.N.B. contributed equally to this manuscript as co-first authors.

Submitted for publication December 21, 2015. Accepted for publication April 28, 2016. From the Department of Anesthesiology (M.S.M., K.C.N., S.M.K.), Geriatric Behavioral Health Division, Department of Psychiatry and Behavioral Sciences, (J.N.B., D.J.M.), Department of Radiology, (T.B.H.), and Duke Brain Imaging and Analysis Center, Duke University Medical Center, Durham, North Carolina (J.N.B., T.B.H., D.J.M.).

 Anesthesiology 2016; 125:368-77

<zdoi;10.1097/ALN.0000000000001198>

of representations adjacent to the blocked area and disinhibition of previously inhibitory connections resulting in increased two-point discrimination acuity. While plasticity has most likely evolved to produce an adaptive response such as this, evidence suggests that maladaptive plasticity may be responsible for phantom limb pain,[11] poor hand rehabilitation,[12,13] and disorders of body schema.[14] Studies have demonstrated that temporary functional deafferentation (TFD) through pharmacologic or ischemic block can promote adaptive brain plasticity in these populations[15–17]; however, interpretation of the findings proves difficult with limited functional imaging studies documenting the effects of TFD in healthy individuals. Despite encouraging results, the details of deafferentation-induced plasticity have not been fully elucidated. This is especially true for plastic changes in healthy subjects after peripheral nerve blocks (PNBs) used for surgical anesthesia.

Research into the effects of PNB on the uninjured brain may provide insight into brain plasticity and its potential role in promoting adaptive changes. While infrequently utilized as an experimental model of TFD, PNB is commonly used in clinical practice to provide surgical anesthesia and postoperative analgesia.[18] PNB is an attractive model to study brain plasticity, because it provides transient deafferentation and deefferentation, allows for timing tailored to local anesthetic duration of action, and overcomes obvious practical limitations (brief time, pain) of ischemia-induced TFD. Increasingly, resting-state functional connectivity (RSFC) and functional connectivity (FC) magnetic resonance imaging (MRI) are being used to study brain activity and organization. Studies to date investigating the effects of TFD through PNB on brain activity in healthy human subjects[19,20] have not investigated the resting-state functional brain network.

RSFC reflects functionally integrated relationships between spatially separated brain regions at rest. It is commonly being utilized to study brain disease and/or damage.[21] Studies utilizing task-driven functional MRI (fMRI) analyses are difficult to accomplish and limited in their application for patients with severe impairment subsequent to disease, nerve injury, stroke, or experimental deafferentation such as the PNB model used in this study. However, ample evidence demonstrates that resting-state networks are stable, are reproducible, and reflect networks associated with cognitive or behavioral task performance.[22–25] Thus, the methodologic advantage of RSFC is that it can be measured without an overt task or external input,[22] and resulting data can be interrogated for individual differences over time and conditions.[26] Indeed, evidence in stroke-affected[27] and nerve-injured subjects[28] suggests that RSFC can serve both as a tool to assess the health of brain networks and as a prognostic indicator of functional recovery.

The purpose of this study was to help determine *in vivo* functional plasticity using RSFC associated with TFD in healthy human participants undergoing PNB. By better understanding the functional neuroanatomical correlates of PNB used in clinical practice, the results of this study may determine if PNB can play a role as a TFD model and ultimately a model for investigating pathologic states.

Material and Methods

This study was approved by the Duke University Medical Center Institutional Review Board. All enrolled study participants provided written informed consent and received financial compensation for study participation.

Participants

The authors recruited participants from an institutional review board–approved flyer advertising the study on the Duke University campus. Ten healthy, right-hand dominant participants (mean age, 22.5 ± 2.6 yr; range, 19 to 28 yr), 7 men and 3 women, were enrolled in this pilot study from August 2009 to May 2012. Racial demographics of the sample consisted of seven non-Hispanic Caucasians, two African Americans and one Asian American participant. Exclusion criteria included standard contraindications to PNB and/or MRI. Participants underwent an anesthetic history and physical exam before active study participation (performed by Dr. Melton).

Procedure

Each participant was scanned during three RSFC experimental conditions: (1) before PNB (pre-PNB), (2) during active PNB (PNB), and (3) during PNB recovery (post-PNB), on a General Electric MR750 3 tesla MRI system (GE Healthcare, United Kingdom) using an eight-channel head coil. In addition to the RSFC experimental conditions, participants' left and right hemispheric sensorimotor regions were empirically determined using a block-design task-based fMRI sequence just before the pre-PNB scanning session. The pre-PNB, active PNB, and post-PNB neuroimaging sessions were conducted on the same day. After pre-PNB RSFC data acquisition, participants were removed from the MRI scanner, and the PNB was performed on the *right* upper extremity in a routine clinical fashion.[29] During PNB, participants were placed supine, with the head of the bed slightly elevated, and the participant's head turned to the contralateral side. After routine, standard monitors were applied, an ultrasound-guided, in-plane supraclavicular nerve block of the brachial plexus was performed using a 22-gauge Stimuplex (B. Braun Medical Inc., USA) needle. Upon ultrasound visualization of appropriate needle to nerve approximation, 30 ml chloroprocaine, 2%, with 1:400k epinephrine and 2 ml sodium bicarbonate, 8.4%, in combined solution was administered incrementally after negative aspiration. This local anesthetic combination has a rapid onset (less than 30 min) and short duration of action (up to 2 h). Before the PNB scan, full motor (0/5) and sensory (absent) blockade of the upper extremity was confirmed by testing motor function (shoulder abduction, elbow flexion/extension, wrist flexion/extension, finger abduction/adduction, and thumb abduction) on a scale of 0 to 5 (0 = no visible

contraction, 1 = visible contraction/no movement, 2 = some movement/cannot overcome gravity, 3 = overcome gravity/not additional force, 4 = less than normal, and 5 = normal) and sensation (pinprick) in the axillary, radial, median, ulnar, and musculocutaneous nerve distributions of the upper extremity in comparison to the nonblocked extremity. This testing was repeated before the post-PNB scan to confirm clinical PNB resolution, as defined by return of full motor strength (5/5) and full sensation to pinprick in the aforementioned nerve distributions as compared to the nonblocked extremity. The duration of motor sensory block was expected to be no more than 2 h. The post-PNB session began at least 2 h after the active PNB data acquisition ended to provide adequate time for clinical PNB recovery.

Within each of the three scanning sessions, resting-state (rs)-fMRI data were collected, with participants being instructed to remain still with their eyes open and visually fixated on a crosshair presented through a back-projected screen that was reflected into a prism mirror affixed to the head coil cage. During the pre-PNB task-based psychomotor fMRI sequence (*i.e.*, motor regions of interest [ROIs] determination sequence), participants were instructed to tap the fingers on either their left or right hand during 20 s alternating equal duration periods of finger tapping or no motor movement. The resulting sensorimotor fMRI activation maps were retained as seed regions for subsequent seed-to-seed and seed-to-voxel RSFC within- and between-condition analyses (see Functional Connectivity Analyses).

Neuroimaging Data Acquisition

Anatomical data were acquired using a high-resolution T1-weighted fast spoiled gradient echo scan (256^2 matrix; field of view, 24 cm; 162 1-mm thick slices; echo time, 3.22 ms; and repetition time, 8,150 ms). Resting-state (rs-fMRI) and pre-PNB motor task-based fMRI data were acquired with a SENSE spiral-in sequence (64^2 matrix; field of view, 24 cm; 34 4-mm thick slices; echo time, 30 ms; repetition time, 2,000 ms; and SENSE factor 2). The rs-fMRI data consisted of 150 time points (5 min) for each experimental condition (pre-PNB, PNB, post-PNB), while 130 time points were collected during the pre-PNB task-based sensorimotor localization fMRI run (4.33 min). Four initial time points (8 s) were discarded from all functional run types to correct for potential, initial magnetic resonance signal instability.

Determination of Right and Left Manual Motor Regions

Task-based, manual motor movement fMRI data were analyzed in SPM (version 8, Wellcome Institute, London). Preprocessing of the functional data included standard slice timing correction and motion correction parameters. Functional and anatomical images were coregistered and then normalized to the Montreal Neurologic Institute (MNI; Montreal, Quebec, Canada) atlas. Group activation maps were created for the right hand and left hand tapping sensorimotor regions by directly contrasting participant motor movement blocks *versus* rest block from the pre-PNB task-based fMRI sequence (see Procedure). After multiple comparison correction thresholding (family-wise error-corrected *P* value less than 0.001), the remaining clusters covering appropriate left and right sensorimotor cortices were saved as group averaged ROIs for inclusion in subsequent seed-to-seed and seed-to-voxel RSFC within- and between-condition data comparisons.

Resting-state fMRI Data

The rs-fMRI data during preblock baseline, during active nerve block (*i.e.*, PNB), and during PNB recovery (*i.e.*, post-PNB) were preprocessed and analyzed with Statistical Parametric Mapping MATLAB software (SPM version 8, Wellcome Institute) with the SPM CONN toolbox (version 15.a).[30] Coregistered T1 anatomical and rs-fMRI data were normalized to MNI common atlas space, and the anatomical data were then segmented to produce gray, white, and cerebrospinal fluid maps for each participant. First-level covariates for each participant's rs-fMRI data included their standard motion parameter time course and time course of artifact detection tool–based "scrubbed" signal artifacts (scan-to-scan global signal z-value threshold more than or equal to 3; composite motion threshold more than or equal to 0.5 mm). Linear regression of confounding effects was then conducted to include cerebrospinal fluid and white matter masked blood oxygen level–dependent (BOLD) time series (aCompCor) and all first-level covariates (*e.g.*, motion correction and "scrubbing"), after which resulting data were band-pass frequency filtered (0.008 to 0.09 Hz). BOLD signal session-specific linear detrending and despiking occurred after confound removal regression.

Band-pass frequency–filtered and postprocessed rs-fMRI BOLD time series were averaged within each empirically defined sensorimotor ROI. Linear FC between these sensorimotor ROIs and between these ROIs and gray matter voxels throughout the cortical and subcortical gray matter and cerebellum was expressed by bivariate correlation analyses of source ROI and target BOLD signal, the results of which were then Fisher z transformed (inverse hyperbolic tangent function) to create subject-/session-specific MNI-spatially normalized ROI-to-ROI and ROI seed-to-voxel RSFC maps.

Analyses

Functional Connectivity Analyses. Random-effects, within-condition, and one-sample paired Student's *t* test analyses of left and right sensorimotor ROI-to-ROI intrinsic connectivity were conducted to assist with visualization of any direct interhemispheric FC changes between these ROIs associated with pre-PNB, PNB, and post-PNB conditions (fig. 1, A and B) and to determine potential pattern differences in RSFC between the sensorimotor ROIs and other gray matter brain regions by condition (table 1; fig. 2, A1.3 and B1.3). Random-effects, between-condition analyses were conducted as a series of independent, one-sample paired Student's *t* tests

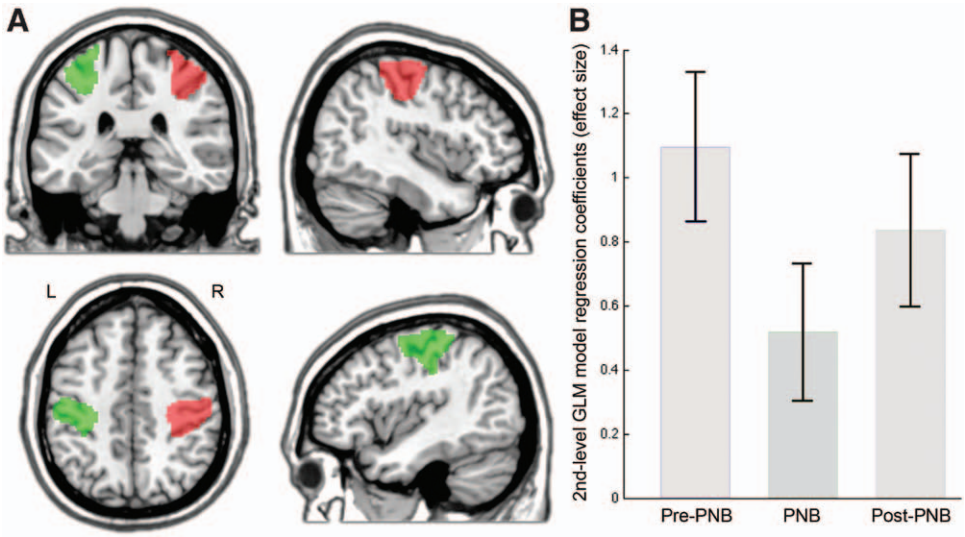

Fig. 1. Comparison of functional connectivity magnitudes between left and right manual motor tapping regions at pre-peripheral nerve block (PNB), during PNB, and after PNB. Random-effects, one-sample Student's *t* tests of first-level left-to-right manual motor tapping regions-of-interest (ROIs) z-transformed bivariate correlation values for each experimental condition. General linear model (GLM) statistical significance threshold peak voxel $P < 0.001$, false discovery rate (FDR) cluster-corrected $P < 0.05$. (*B*) Y-axis values denote the effect size of intrinsic functional connectivity (expressed as mean ROI Fisher transformed *r* values) between left (L; *green* region; *A*) and *right* (R; *red* region; *A*) manual motor regions during each experimental condition (*i.e.*, pre-peripheral nerve block [pre-PNB], during peripheral nerve block [PNB], and after nerve block resolution [post-PNB]). *Error bars* reflect parameter estimate 90% CIs.

of regression differences in sensorimotor ROI seed-to-voxel FC maps between pre-PNB and PNB, post-PNB (*i.e.*, during PNB recovery) and PNB, and pre-PNB and post-PNB conditions (table 2; fig. 3, A–D). All analyses were conducted with statistical thresholds set to multiple-comparison–corrected, false discovery rate–corrected *P* value less than 0.05 for the within-condition sensorimotor ROI-to-ROI analyses and to a voxel peak $P < 0.001$ and cluster extent (k_E) false discovery rate–corrected *P* value less than 0.05 for the within-condition and between-condition ROI seed-to-voxel analyses. Reported effect sizes (β) are expressed as either within-condition Fisher-z–transformed standardized regression coefficients or between-condition standardized regression coefficient differences, depending upon the analyses type.

Results

ROI-to-ROI Sensorimotor between-condition RSFC Analyses

ROI-to-ROI sensorimotor RSFC analyses demonstrated significant changes in interhemispheric correlation between the left and right group-averaged sensorimotor and primary motor cortex ROIs (fig. 1A) across the pre-PNB, PNB, and post-PNB sessions. Before PNB placement (pre-PNB), the sensorimotor ROIs showed very strong interhemispheric RSFC (β = 1.05; fig. 1B, bar 1). After PNB placement (PNB), while interhemispheric RSFC after behavioral PNB recovery was significantly reduced (by approximately half of the pre-PNB connectivity magnitude; β = 0.55), bilateral intrahemispheric RSFC was maintained (fig. 1B, bar 2), and upon behavioral recovery of PNB (post-PNB), interhemispheric ROI-to-ROI RSFC returned close to pre-PNB values (β = 0.82; fig. 1B, bar 3).

Sensorimotor ROI Seed-to-voxel within-condition RSFC Analyses

Before PNB, the left sensorimotor ROI seed region was positively associated with a statistically significant large gray matter intra- and interhemispheric region in the left and right pre- and postcentral somatosensory and primary cortices (t = 26.54, β = 0.61), as well as regions in right tertiary visual cortex (V3; t = 11.81, β = 0.29) and left somatosensory association cortex (t = 7.45, β = 0.26; fig. 2A.1 and table 1). Similar regions of RSFC association were found for the right sensorimotor ROI seed. The right hemisphere ROI shared intrinsic FC with left and right somatosensory and primary cortices (t = 25.12, β = 0.62) and an intrahemispheric region in the tertiary visual cortex (V3, t = 9.72, β = 0.28; fig. 2B.1 and table 1). For both the left and right sensorimotor ROI seeds, the highest degree of FC association was found with respective proximal intrahemispheric sensorimotor regions, but as demonstrated in the direct ROI-to-ROI analyses, significant interhemispheric connectivity of homologous motor and primary sensory regions was observed for both seeds before PNB.

During active PNB, intrahemispheric RSFC did not change appreciably with each of the sensorimotor seed regions showing a general preservation of localized RSFC within each hemisphere, but the interhemispheric RSFC between primary motor and sensory regions was adversely

Table 1. Left and Right Sensorimotor Intrinsic Functional Connectivity Networks at Pre-PNB, during PNB, and after PNB

Seed/ROI*	Condition	Locus Region(s) *(Brodmann Areas)*†	$SPM_{(T)}$	k_E	β‡	Local Maxima§ x	y	z
Left motor region	Pre-PNB	L/R. pre-/postcentral gyrus (1, 4)	26.54	12,850	0.61	−48	−22	60
		R. inferior lateral occipital cortex (19)	11.81	455	0.29	44	−72	−2
		L. superior lateral occipital/cuneus (7)	7.45	133	0.26	−24	−72	30
	PNB	L. pre-/postcentral gyrus (1, 4)	26.33	5,932	0.67	−32	−36	60
		L. midinsular cortex (13)	12.49	239	0.28	−32	−2	10
		R. postcentral gyrus (1)	8.15	1,251	0.42	54	−20	34
	Post-PNB	L. pre-/postcentral gyrus (1, 4)	32.98	5,791	0.70	−36	−36	60
		R. postcentral gyrus (1)	15.62	2,198	0.52	44	−30	48
		L. inferior lateral occipital cortex (19)	14.47	1,249	0.25	−46	−80	4
		R. inferior lateral occipital cortex (19)	13.58	1,190	0.26	48	−78	10
		R. cerebellar regions 4, 5/lingual gyrus	11.90	926	0.25	12	−52	−18
		L. cerebellar regions 4,5,6	8.39	138	0.17	−18	−54	−30
Right motor region	Pre-PNB	R/L. pre-/postcentral gyrus (1, 4)	25.12	11,533	0.62	36	−34	58
		R. inferior lateral occipital cortex (19)	9.72	407	0.28	44	−76	−4
	PNB	R. pre-/postcentral gyrus and insula (1, 4, 13)	34.61	8,219	0.62	26	−14	72
		L. postcentral and superior parietal cortex (5)	8.10	711	0.40	−26	−36	50
	Post-PNB	R. pre-/postcentral gyrus (1, 4)	22.81	6,644	0.70	46	−26	62
		L. cerebellar regions 4, 5, 6/TOFusC	11.13	498	0.25	−10	−52	−14
		L. pre-/postcentral gyrus (1, 4)	8.74	3,531	0.51	−34	−10	60
		R. cerebellar regions 4, 5, 6/TOFusC	6.47	192	0.20	22	−48	−20
		R. inferior lateral occipital cortex (19)	6.37	657	0.31	50	−76	10
		R. superior lateral occipital/cuneus (18)	5.18	141	0.16	16	−80	24

*Statistical parametric mapping (SPM) second-level, one-sample Student's *t* test comparisons of seed-to-voxel resting-state functional magnetic resonance imaging intrinsic connectivity associated with motor ROIs within experimental conditions (peak voxel threshold $P < 0.001$, cluster spatial extent (k_E; expressed in volume) threshold p-false discovery rate < 0.05). See figure 2 for visualization of locus region(s) by motor seed and condition. †Anatomical and Brodmann area labels based upon 7-mm^3 search range of the Talairach Daemon Database[31] using Montreal Neurologic Institute (MNI)-to-Talairach nonlinear transform coordinates. ‡Effect size (β expressed as Fisher-z–transformed standardized regression coefficients). §MNI International Consortium for Brain Mapping 152 nonlinear sixth-generation brain atlas coordinates.[32]

PNB = peripheral nerve block; post-PNB = after peripheral nerve block resolution; pre-PNB = before peripheral nerve block; ROI = region of interest; TOFusC = temporal occipital fusiform cortex.

affected by PNB administration. RSFC with the left sensorimotor ROI was proximally associated with gray matter regions in the intrahemispheric somatosensory and primary motor cortices (t = 26.33, β = 0.67) and a smaller region in the insular cortex (t = 12.49, β = 0.28; fig. 2A.2). The only region of interhemispheric RSFC with the left sensorimotor ROI was a region in the right somatosensory cortex, but as with the ROI-to-ROI analyses, the magnitude and cortical spatial area of the association was significantly reduced during PNB (*e.g.*, pre-PNB: t = 26.54, β = 0.61 *vs.* PNB: t = 8.15, β = 0.42; table 1). RSFC association with the right sensorimotor ROI evinced a similar pattern of preserved intrahemispheric connectivity proximal to the primary motor and somatosensory cortices and insular cortex (t = 34.61, β = 0.62) and a smaller region of interhemispheric connectivity with the left somatosensory cortex (t = 8.10, β = 0.40; fig. 2B.2 and table 1).

After observational and behavioral PNB recovery, participants were rescanned, and RSFC associated with our left and right sensorimotor seeds was once again examined. Left and right motor seed regions strengthened their interhemispheric RSFC from the active PNB state, but not to the same extent as seen in pre-PNB (fig. 2, A.3 and B.3; table 1). In addition to the relative resumption of interhemispheric sensorimotor intrinsic FC, it was observed that there were additional bilateral cerebellum (regions 4 and 5) and tertiary visual cortex regions showing RSFC with the motor seeds that were not observed during pre-PNB or during active PNB for either of the sensorimotor seed ROIs (fig. 2, A.3 and B.3; table 1).

Sensorimotor ROI Seed-to-voxel between-condition RSFC Analyses

Direct comparison of pre-PNB, active PNB, and post-PNB conditions by motor seed region highlighted the observed significant diminishment of RSFC between interhemispheric motor regions during PNB between left and right motor seeds relative to pre-PNB FC (left to right: t = 10.99, β = 0.33; right to left: t = 10.45, β = 0.40; table 2; fig. 3, A and B). Additionally, it was observed that intrahemispheric RSFC between the left motor seed and superior lateral occipital cortex was significantly greater at pre-PNB baseline (t = 8.41, β = 0.23; fig. 3A). There were no areas of statistically significant RSFC increase during PNB relative to pre-PNB for either of the sensorimotor ROIs. Comparisons of PNB and post-PNB conditions were associated with only a single region of increased FC strength during active PNB relative to post-PNB for the right motor seed (*i.e.*, right posterior supramarginal gyrus, t = 6.39, β = 0.29; table 2; fig. 3C). As

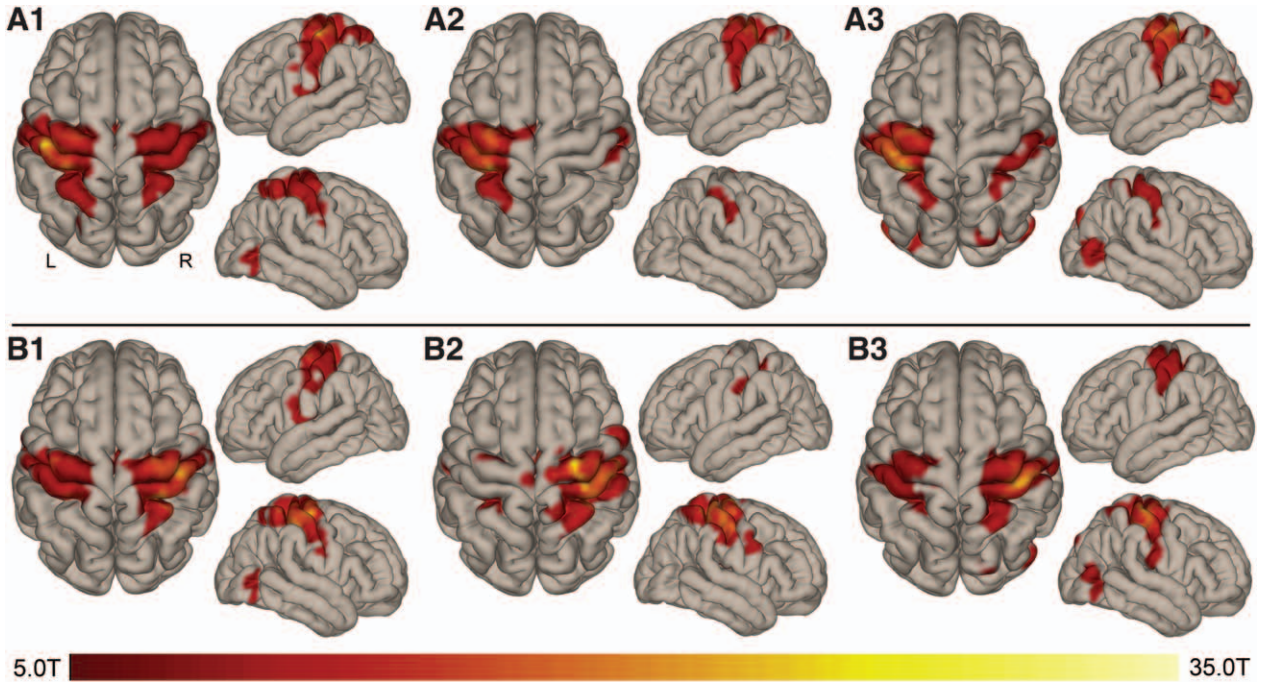

Fig. 2. Left and right hemisphere motor region-of-interest (ROI) seed-to-voxel whole brain functional connectivity at pre-peripheral nerve block (PNB), during PNB, and after PNB. Random-effects, group-wise independent one-sample Student's *t* tests of subject-specific first-level seed-to-voxel connectivity maps by condition. Statistical significance established as peak voxel $P < 0.001$ and multiple-comparison corrected cluster false discovery rate $P < 0.05$. Whole brain seed-to-voxel intrinsic functional connectivity analyses reflect regions of significant, confound-removed blood oxygen level–dependent (BOLD) time series signal correlation with mean BOLD time series signal within predefined ROIs; in this case, the mean BOLD time series signal within the left and right manual motor regions is shown in figure 1. Colored areas reflect the spatial location of cortical regions with significantly associated time series signal with the left manual motor region seed ROI at pre-PNB (*A1*), during PNB (*A2*), and after PNB resolution (post-PNB; *A3*), while associated cortical regions with shared BOLD time series signal characteristics to the right manual motor region seed ROI are visualized at pre-PNB (*B1*), PNB (*B2*), and post-PNB (*B3*). The *red–yellow bar* denotes peak voxel statistical significance in t values above the $P < 0.001$ threshold.

Table 2. Intrinsic Functional Connectivity Differences of Left and Right Sensorimotor ROIs between Experimental Conditions

Seed/ROI*	Significant Contrasts	Locus Region(s) *(Brodmann Areas)*†	$SPM_{\{T\}}$	k_E	β‡	Local Maxima§ x	y	z
Left motor region	Pre-PNB > PNB	R. pre-/postcentral gyrus (1, 4, 6)	10.99	1,581	0.33	26	−14	64
		L. sup. lat. occipital cortex (19)	8.41	138	0.23	−22	−70	22
	Post-PNB > PNB	L/R. ventral posterior cingulate (23)	11.86	1,388	0.25	0	−60	18
		R. sup. lat. occipital cortex (19)	8.47	280	0.25	24	−84	34
		L. inf. lat. occipital cortex (18)	8.32	209	0.21	−38	−80	6
		R. lingual gyrus (18)	7.64	136	0.23	12	−70	−6
		L. lingual gyrus (19)	7.00	125	0.23	−16	−60	−12
Right motor region	Pre-PNB > PNB	L. pre-/postcentral gyrus (4, 6)	10.45	968	0.40	−26	−18	70
	PNB > Post-PNB	R. pos. supramarginal gyrus (40)	6.39	226	0.29	54	−46	56
		r						

*Statistical parametric mapping (SPM) second-level, paired Student's *t* test comparison of voxel-wise resting-state functional magnetic resonance imaging intrinsic connectivity associated with motor ROI seeds between experimental conditions (peak voxel threshold $P < 0.001$, cluster spatial extent (k_E; expressed in voxel volume) threshold p-false discovery rate < 0.05). See figure 3 for visualization of locus region(s) by motor seed between PNB conditions. †Anatomical and Brodmann area labels based upon 7-mm^3 search range of the Talairach Daemon Database[31] using Montreal Neurologic Institute (MNI)-to-Talairach nonlinear transform coordinates. ‡Effect size (expressed as the difference in Fisher-z–transformed standardized regression coefficients between conditions). §MNI International Consortium for Brain Mapping 152 nonlinear sixth-generation brain atlas coordinates.[32]

inf. lat. = inferior lateral; PNB = peripheral nerve block; pos. = posterior; post-PNB = after peripheral nerve block resolution; pre-PNB = before peripheral nerve block; ROI = region of interest; sup. lat. = superior lateral.

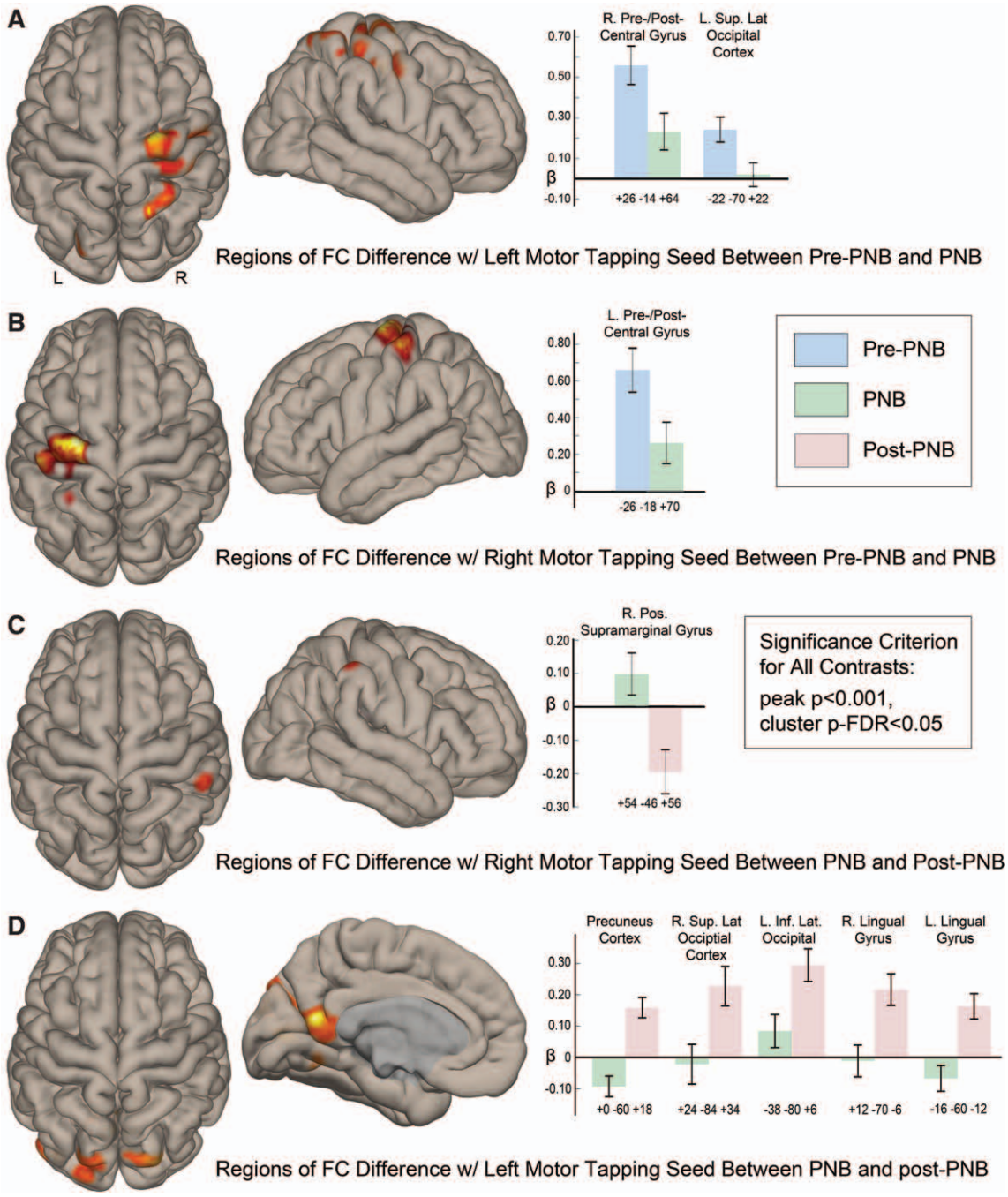

Fig. 3. Regions of significant whole brain functional connectivity change with left and right manual motor tapping regions between pre-peripheral nerve block (PNB), during PNB, and after PNB conditions. Random-effects, paired Student's *t* test contrasts of seed-to-voxel intrinsic functional connectivity (FC) differences for left and right manual motor regions (fig. 1) between pre-PNB, during active PNB, and after PNB resolution (post-PNB) conditions. Statistical significance established as peak voxel $P < 0.001$ and multiple-comparison corrected cluster false discovery rate $P < 0.05$. (*A*) The spatial locations and effect size differences for brain regions demonstrating a significant difference in intrinsic FC with the left manual motor region during pre-PNB (*blue bars*) relative to the PNB (*green bars*) condition, while (*B*) reflects regions of difference between the same conditions for the right manual motor region. (*C*) The spatial location and effect size of condition-wise differences between PNB (*green bars*) and post-PNB (*pink bars*) for the right manual motor region; (*D*) significant regions of difference and their associated effect sizes between the PNB and post-PNB conditions for the left manual motor region. Y-axis β values reflect standardized Fisher r value–transformed differences between conditions for each significant seed-to-voxel cluster (*i.e.*, condition-wise effect sizes). *Error bars* reflect parameter estimate 90% CIs. Montreal Neurologic Institute coordinates below each set of *condition bars* are the spatial location of the cluster maxima in each significant seed-to-voxel cluster, while verbal descriptors of the cluster maxima spatial location are given above each set of condition *contrast bars*.

noted in our within-condition examination of ROI seed-to-voxel RSFC after behavioral recovery of PNB (post-PNB), there were numerous regions in the primary and secondary visual cortices that were observed to have greater RSFC with the left sensorimotor ROI during PNB recovery than during active PNB (*e.g.*, precuneus, right/left lateral occipital cortices, and right/left lingual gyrus regions; table 2, fig. 3D). No regions exceeded multiple comparison correction statistical thresholds of direct contrasts between pre-PNB and post-PNB conditions for the left and right motor seeds.

Discussion

This study investigated the effects of TFD through supraclavicular PNB on regional and global RSFC (*i.e.*, intrinsic FC) in healthy human participants before PNB, during active PNB, and during PNB recovery. The results demonstrated transient disruption of *inter*hemispheric RSFC of the left and right manual motor regions but preservation of *intra*hemispheric RSFC of these regions during PNB. Additionally, there was increased RSFC between the left motor ROI (PNB-affected area) and *bilateral* higher order visual cortex regions (precuneus, lingual gyrus, and superior lateral occipital cortex) after behavioral PNB recovery. These results illustrate the *in vivo* changes occurring in sensorimotor functional brain networks during PNB as used in clinical practice and provide evidence that PNB has features consistent with other models of deafferentation, making it a potentially useful approach to investigate interhemispheric plasticity.

Preservation of *intra*hemispheric intrinsic connectivity is in accordance with previous studies in deafferentated rats subsequent to brachial plexus transection[33] and deafferentated humans after brachial plexus injury,[34] stroke,[27] or surgical transection of the corpus callosum (callosotomy).[35] The current study, however, demonstrated for the first time in healthy human adults that *inter*hemispheric plasticity can be induced in the RSFC brain network utilizing deafferentation through a transient and reversible PNB model used in clinical practice and subsequently imaged utilizing fMRI. Additionally, these results suggest that induced *inter*hemispheric plasticity may extend beyond the clinically detected duration of TFD. In light of recent evidence in stroke-affected[27,36] and nerve-injured patients[28,37] demonstrating RSFC to be a predictor of functional recovery and outcome, this model may prove extremely useful to further evaluate this relationship in both healthy and stroke-affected or nerve-injured individuals. Ongoing research by the authors is investigating whether measures of induced plasticity associated with PNB may provide additional prognostic value in neurologically impaired subjects.

This study and others utilizing fMRI are proving to elucidate interhemispheric networks, the associations and interactions therein, and the result of injury to such networks on functional outcome. For example, Van Meer *et al.*[36] demonstrated that functional recovery after stroke is associated with extensive functional and structural remodeling throughout the bilateral sensorimotor network. This included reinstatement of interhemispheric neuronal signal synchronization. Corbetta *et al.*[38] provided evidence that interhemispheric imbalance of task-driven responses is observed at the acute stage after stroke and correlates with visual neglect. Carter *et al.*[27] were able to demonstrate that RSFC between homologous regions of each hemisphere was predictive of behavioral output and arm function during a task in stroke-affected subjects. Finally, Grefkes *et al.*[39] utilizing fMRI demonstrated that subcortical strokes are associated with decrements in interhemispheric neuronal coupling at rest, increased interhemispheric inhibition onto the affected M1 motor cortex during paretic hand movement, and decreased interhemispheric facilitation during bilateral hand movement.

These findings are exploiting maladaptive plasticity and identifying potential targets for neuromodulatory intervention. For example, TFD of the unaffected hand has been proposed to disrupt interhemispheric inhibition onto the affected M1 motor cortex, optimizing plasticity for rehabilitation of paretic hand function subsequent to stroke.[40,41] Results of the current study support the mechanism upon which others have previously proposed to explain functional and/or behavioral correlates of TFD, including alterations of body schema,[20,42] enhanced hand sensorimotor activation/function,[43] and improved rehabilitation subsequent to stroke[12,44] or peripheral nerve injury.[17] This study documents disengagement of preexisting transcallosal interhemispheric inhibitory connections between homologous motor cortices after TFD through PNB. Both anatomic and functional explanations support these finding. Anatomically, homologous regions of the primary motor cortices (M1s) are connected through transcallosal fibers, and these fibers are inherently inhibitory. And, functionally, interhemispheric communication between the two M1s plays a major role in the control of unilateral hand movements, and the strength of this connection seems to be dependent on arm activity.[45] Currently, the authors are investigating the idea of neurointerventional regional anesthesia as a rehabilitative intervention to promote adaptive plasticity for hand paresis rehabilitation in stroke-affected and or nerve-injured individuals.

During PNB recovery, there was enhanced interhemispheric connectivity from the block-affected motor hemisphere to bilateral higher order, motor–visual processing regions known to be associated with body schema, semantic memory for manual skills (*e.g.*, tool use), and the perception of body parts.[46] While clinically and behaviorally participants demonstrated block resolution, subclinical deafferentation may have persisted. Nonetheless, this enhanced connectivity during PNB recovery suggests dependence on these areas to reintegrate the affected or "missing" limb. This finding supports the investigation by Silva *et al.*,[20] which sought to objectively assess the effects of acute deafferentation produced by regional anesthesia on central sensorimotor representations using a visual left/right hand judgment task. Silva *et al.*[20]

speculated that the occurrence of perceptive illusions and impaired hand recognition performance might result from functional disturbances in sensorimotor representations as the consequence of the conflicting persistence of feed-forward motor commands in the absence of proprioceptive and visual feedback. Results of the current study support modulation of the sensory–motor integration feedback loop as Silva *et al.*[20] concluded. Previous studies have demonstrated relationships between deafferentation, vision, and body schema. Induced postural illusions in amputees using mirrors have allowed the absent limb to be "reconstructed" from sight,[36] and chronically deafferentated limbs after brachial plexus injury become "passive entities" excluded from body image,[19,38,39] despite visual input. Increased interhemispheric connectivity to higher order visual cortex areas known to be responsible for sensory–motor integration,[47–50] including the precuneus, lingual gyrus, and superior lateral occipital cortex, as demonstrated in this study, may provide greater insight into these findings.

There are limitations associated with this study. While supraclavicular PNB is commonly utilized in clinical practice and minimally invasive to perform, given the potential risks and transient side effects associated with their use, we limited the number of participants in this volunteer, nonsurgical population. This was a pilot study; as such there was no power analysis for a defined primary outcome. Although the sample size is similar to comparable studies, future longitudinal studies involving larger groups of subjects at various points along the aging spectrum are warranted. Additionally, previous work has questioned whether local anesthetic plasma levels associated with PNB could induce neuroplasticity.[20] While local anesthetics readily cross the blood–brain barrier,[51] it is unlikely that plasma concentrations associated with peripheral administration of chloroprocaine, which is rapidly metabolized, through PNB[52] produced pharmacologically active brain exposure to confound the mechanism of neuroplasticity in this study.

This study demonstrated for the first time in human participants, utilizing a PNB model, that TFD disrupted interhemispheric intrinsic connectivity between homologous motor regions, while preserving *intra*hemispheric connectivity. Additionally, intrinsic FC increased from the block-affected motor hemisphere to bilateral higher order, motor–visual processing regions associated with body schema, semantic memory for manual skills, and the perception of body parts, which persisted beyond the behavioral duration of TFD. Interhemispheric connectivity plays a critical role in brain function. As such, induced plasticity of interhemispheric networks has significant experimental and clinical implications. TFD through PNB presents an attractive intervention to modulate interhemispheric neuroplasticity for future research and/or possible clinical application.

Research Support

This research was supported in part by institutional and departmental sources, as well as by National Institutes of Health (Bethesda, Maryland) research grants R21 HL109971 (to Drs. Browndyke and Harshbarger), R01 AG039684 (to Dr. Madden), and R01 MH098301 (to Dr. Madden).

Competing Interests

The authors declare no competing interests.

Reproducible Science

Full protocol available from Dr. Melton: steve.melton@duke.edu.
Raw data available from Dr. Melton: steve.melton@duke.edu.

Correspondence

Address correspondence to Dr. Melton: Duke University Medical Center, DUMC #3094 Stop #4, Durham, North Carolina 27710. steve.melton@duke.edu. This article may be accessed for personal use at no charge through the Journal Web site, www.anesthesiology.org.

References

1. Merzenich MM, Kaas JH, Wall JT, Sur M, Nelson RJ, Felleman DJ: Progression of change following median nerve section in the cortical representation of the hand in areas 3b and 1 in adult owl and squirrel monkeys. Neuroscience 1983; 10:639–65
2. Merzenich MM, Kaas JH, Wall J, Nelson RJ, Sur M, Felleman D: Topographic reorganization of somatosensory cortical areas 3b and 1 in adult monkeys following restricted deafferentation. Neuroscience 1983; 8:33–55
3. Merzenich MM, Nelson RJ, Stryker MP, Cynader MS, Schoppmann A, Zook JM: Somatosensory cortical map changes following digit amputation in adult monkeys. J Comp Neurol 1984; 224:591–605
4. Wall JT, Kaas JH, Sur M, Nelson RJ, Felleman DJ, Merzenich MM: Functional reorganization in somatosensory cortical areas 3b and 1 of adult monkeys after median nerve repair: Possible relationships to sensory recovery in humans. J Neurosci 1986; 6:218–33
5. Metzler J, Marks PS: Functional changes in cat somatic sensory-motor cortex during short-term reversible epidural blocks. Brain Res 1979; 177:379–83
6. Rossini PM, Martino G, Narici L, Pasquarelli A, Peresson M, Pizzella V, Tecchio F, Torrioli G, Romani GL: Short-term brain 'plasticity' in humans: Transient finger representation changes in sensory cortex somatotopy following ischemic anesthesia. Brain Res 1994; 642:169–77
7. Werhahn KJ, Mortensen J, Kaelin-Lang A, Boroojerdi B, Cohen LG: Cortical excitability changes induced by deafferentation of the contralateral hemisphere. Brain 2002; 125 (pt 6):1402–13
8. Levy LM, Ziemann U, Chen R, Cohen LG: Rapid modulation of GABA in sensorimotor cortex induced by acute deafferentation. Ann Neurol 2002; 52:755–61
9. Weiss T, Miltner WH, Liepert J, Meissner W, Taub E: Rapid functional plasticity in the primary somatomotor cortex and perceptual changes after nerve block. Eur J Neurosci 2004; 20:3413–23
10. Ziemann U, Hallett M, Cohen LG: Mechanisms of deafferentation-induced plasticity in human motor cortex. J Neurosci 1998; 18:7000–7
11. Karl A, Birbaumer N, Lutzenberger W, Cohen LG, Flor H: Reorganization of motor and somatosensory cortex in upper extremity amputees with phantom limb pain. J Neurosci 2001; 21:3609–18
12. Floel A, Hummel F, Duque J, Knecht S, Cohen LG: Influence of somatosensory input on interhemispheric interactions in patients with chronic stroke. Neurorehabil Neural Repair 2008; 22:477–85
13. Rosén B, Björkman A, Lundborg G: Improved sensory relearning after nerve repair induced by selective temporary

anaesthesia—A new concept in hand rehabilitation. J Hand Surg Br 2006; 31:126–32
14. Bromage PR, Melzack R: Phantom limbs and the body schema. Can Anaesth Soc J 1974; 21:267–74
15. Birbaumer N, Lutzenberger W, Montoya P, Larbig W, Unertl K, Töpfner S, Grodd W, Taub E, Flor H: Effects of regional anesthesia on phantom limb pain are mirrored in changes in cortical reorganization. J Neurosci 1997; 17:5503–8
16. Voller B, Flöel A, Werhahn KJ, Ravindran S, Wu CW, Cohen LG: Contralateral hand anesthesia transiently improves post-stroke sensory deficits. Ann Neurol 2006; 59:385–8
17. Björkman A, Rosén B, van Westen D, Larsson EM, Lundborg G: Acute improvement of contralateral hand function after deafferentation. Neuroreport 2004; 15:1861–5
18. Klein SM, Evans H, Nielsen KC, Tucker MS, Warner DS, Steele SM: Peripheral nerve block techniques for ambulatory surgery. Anesth Analg 2005; 101:1663–76
19. Björkman A, Rosén B, Lundborg G: Anaesthesia of the axillary plexus induces rapid improvement of sensory function in the contralateral hand: An effect of interhemispheric plasticity. Scand J Plast Reconstr Surg Hand Surg 2005; 39:234–7
20. Silva S, Loubinoux I, Olivier M, Bataille B, Fourcade O, Samii K, Jeannerod M, Démonet JF: Impaired visual hand recognition in preoperative patients during brachial plexus anesthesia: Importance of peripheral neural input for mental representation of the hand. Anesthesiology 2011; 114:126–34
21. Fox MD, Greicius M: Clinical applications of resting state functional connectivity. Front Syst Neurosci 2010; 4:19
22. Park CH, Chang WH, Ohn SH, Kim ST, Bang OY, Pascual-Leone A, Kim YH: Longitudinal changes of resting-state functional connectivity during motor recovery after stroke. Stroke 2011; 42:1357–62
23. Bianciardi M, Fukunaga M, van Gelderen P, Horovitz SG, de Zwart JA, Duyn JH: Modulation of spontaneous fMRI activity in human visual cortex by behavioral state. Neuroimage 2009; 45:160–8
24. Fox MD, Snyder AZ, Vincent JL, Corbetta M, Van Essen DC, Raichle ME: The human brain is intrinsically organized into dynamic, anticorrelated functional networks. Proc Natl Acad Sci USA 2005; 102:9673–8
25. Buckner RL: Human functional connectivity: New tools, unresolved questions. Proc Natl Acad Sci USA 2010; 107:10769–70
26. Mennes M, Kelly C, Zuo XN, Di Martino A, Biswal BB, Castellanos FX, Milham MP: Inter-individual differences in resting-state functional connectivity predict task-induced BOLD activity. Neuroimage 2010; 50:1690–701
27. Carter AR, Astafiev SV, Lang CE, Connor LT, Rengachary J, Strube MJ, Pope DL, Shulman GL, Corbetta M: Resting interhemispheric functional magnetic resonance imaging connectivity predicts performance after stroke. Ann Neurol 2010; 67:365–75
28. Klingner CM, Volk GF, Brodoehl S, Burmeister HP, Witte OW, Guntinas-Lichius O: Time course of cortical plasticity after facial nerve palsy: A single-case study. Neurorehabil Neural Repair 2012; 26:197–203
29. Chan VW, Perlas A, Rawson R, Odukoya O: Ultrasound-guided supraclavicular brachial plexus block. Anesth Analg 2003; 97:1514–7
30. Whitfield-Gabrieli S, Nieto-Castanon A: Conn: A functional connectivity toolbox for correlated and anticorrelated brain networks. Brain Connect 2012; 2:125–41
31. Lancaster JL, Woldorff MG, Parsons LM, Liotti M, Freitas CS, Rainey L, Kochunov PV, Nickerson D, Mikiten SA, Fox PT: Automated Talairach atlas labels for functional brain mapping. Hum Brain Mapp 2000; 10:120–31
32. Tzourio-Mazoyer N, Landeau B, Papathanassiou D, Crivello F, Etard O, Delcroix N, Mazoyer B, Joliot M: Automated anatomical labeling of activations in SPM using a macroscopic anatomical parcellation of the MNI MRI single-subject brain. Neuroimage 2002; 15:273–89
33. Pawela CP, Biswal BB, Hudetz AG, Li R, Jones SR, Cho YR, Matloub HS, Hyde JS: Interhemispheric neuroplasticity following limb deafferentation detected by resting-state functional connectivity magnetic resonance imaging (fcMRI) and functional magnetic resonance imaging (fMRI). Neuroimage 2010; 49:2467–78
34. Liu B, Li T, Tang W-J, Zhang J-H, Sun H-P, Xu W-D, Liu H-Q, Feng X-Y: Changes of inter-hemispheric functional connectivity between motor cortices after brachial plexuses injury: A resting-state fMRI study. Neuroscience 2013 243:33–9
35. Johnston JM, Vaishnavi SN, Smyth MD, Zhang D, He BJ, Zempel JM, Shimony JS, Snyder AZ, Raichle ME: Loss of resting interhemispheric functional connectivity after complete section of the corpus callosum. J Neurosci 2008; 28:6453–8
36. van Meer MP, van der Marel K, Wang K, Otte WM, El Bouazati S, Roeling TA, Viergever MA, Berkelbach van der Sprenkel JW, Dijkhuizen RM: Recovery of sensorimotor function after experimental stroke correlates with restoration of resting-state interhemispheric functional connectivity. J Neurosci 2010; 30:3964–72
37. Klingner CM, Volk GF, Maertin A, Brodoehl S, Burmeister HP, Guntinas-Lichius O, Witte OW: Cortical reorganization in Bell's palsy. Restor Neurol Neurosci 2011; 29:203–14
38. Corbetta M, Kincade MJ, Lewis C, Snyder AZ, Sapir A: Neural basis and recovery of spatial attention deficits in spatial neglect. Nat Neurosci 2005; 8:1603–10
39. Grefkes C, Nowak DA, Eickhoff SB, Dafotakis M, Küst J, Karbe H, Fink GR: Cortical connectivity after subcortical stroke assessed with functional magnetic resonance imaging. Ann Neurol 2008; 63:236–46
40. Floel A, Hummel F, Duque J, Knecht S, Cohen LG: Influence of somatosensory input on interhemispheric interactions in patients with chronic stroke. Neurorehabil Neural Repair 2008; 22:477–85
41. Voller B, Flöel A, Werhahn KJ, Ravindran S, Wu CW, Cohen LG: Contralateral hand anesthesia transiently improves post-stroke sensory deficits. Ann Neurol 2006; 59:385–8
42. Paqueron X, Leguen M, Rosenthal D, Coriat P, Willer JC, Danziger N: The phenomenology of body image distortions induced by regional anaesthesia. Brain 2003; 126(pt 3):702–12
43. Kurabe S, Itoh K, Matsuzawa H, Nakada T, Fujii Y: Expansion of sensorimotor cortical activation for unilateral hand motion during contralateral hand deafferentation. Neuroreport 2014; 25:435–9
44. Weiss T, Sens E, Teschner U, Meissner W, Preul C, Witte OW, Miltner WH: Deafferentation of the affected arm: A method to improve rehabilitation? Stroke 2011; 42:1363–70
45. Avanzino L, Bassolino M, Pozzo T, Bove M: Use-dependent hemispheric balance. J Neurosci 2011; 31:3423–8
46. Astafiev SV, Stanley CM, Shulman GL, Corbetta M: Extrastriate body area in human occipital cortex responds to the performance of motor actions. Nat Neurosci 2004; 7:542–8
47. Wolpert DM, Goodbody SJ, Husain M: Maintaining internal representations: The role of the human superior parietal lobe. Nat Neurosci 1998; 1:529–33
48. Castiello U: The neuroscience of grasping. Nat Rev Neurosci 2005; 6:726–36
49. Buneo CA, Andersen RA: The posterior parietal cortex: Sensorimotor interface for the planning and online control of visually guided movements. Neuropsychologia 2006; 44:2594–606
50. Christensen MS, Grey MJ: Modulation of proprioceptive feedback during functional electrical stimulation: An fMRI study. Eur J Neurosci 2013; 37:1766–78
51. Ferrari L, Crestan V, Sabattini G, Vinco F, Fontana S, Gozzi A: Brain penetration of local anaesthetics in the rat: Implications for experimental neuroscience. J Neurosci Methods 2010; 186:143–9
52. Vanterpool S, Steele SM, Nielsen KC, Tucker M, Klein SM: Combined lumbar-plexus and sciatic-nerve blocks: An analysis of plasma ropivacaine concentrations. Reg Anesth Pain Med 2006; 31:417–21